



HAL
open science

Optimal choice of Hankel-block-Hankel matrix shape in 2-D parameter estimation: the rank-one case

Souleymen Sahnoun, Konstantin Usevich, Pierre Comon

► To cite this version:

Souleymen Sahnoun, Konstantin Usevich, Pierre Comon. Optimal choice of Hankel-block-Hankel matrix shape in 2-D parameter estimation: the rank-one case. EUSIPCO 2016 - 24th European Signal Processing Conference, Aug 2016, Budapest, Hungary. hal-01288994v2

HAL Id: hal-01288994

<https://hal.science/hal-01288994v2>

Submitted on 6 Jul 2016

HAL is a multi-disciplinary open access archive for the deposit and dissemination of scientific research documents, whether they are published or not. The documents may come from teaching and research institutions in France or abroad, or from public or private research centers.

L'archive ouverte pluridisciplinaire **HAL**, est destinée au dépôt et à la diffusion de documents scientifiques de niveau recherche, publiés ou non, émanant des établissements d'enseignement et de recherche français ou étrangers, des laboratoires publics ou privés.

Optimal choice of Hankel-block-Hankel matrix shape in 2-D parameter estimation: the rank-one case

Souleymen Sahnoun, Konstantin Usevich, Pierre Comon

Abstract—In this paper we analyse the performance of 2-D ESPRIT method for estimating parameters of 2-D superimposed damped exponentials. 2-D ESPRIT algorithm is based on low-rank decomposition of a Hankel-block-Hankel matrix that is formed by the 2-D data. Through a first-order perturbation analysis, we derive closed-form expressions for the variances of the complex modes, frequencies and damping factors estimates in the 2-D single-tone case. This analysis allows to define the optimal parameters used in the construction of the Hankel-block-Hankel matrix. A fast algorithm for calculating the SVD of Hankel-block-Hankel matrices is also used to enhance the computational complexity of the 2-D ESPRIT algorithm.

Index Terms—Frequency estimation, Hankel-block-Hankel matrix, 2-D ESPRIT, perturbation analysis.

I. INTRODUCTION

High resolution parameter estimation of bidimensional (2-D) and multidimensional signals finds many applications in signal processing and communications such as radar imaging, wireless communications [1], and nuclear magnetic resonance (NMR) spectroscopy [2].

a) State of art: To deal with this problem, several methods have been proposed. They include (i) linear prediction-based methods such as 2-D TLS-Prony [3], (ii) subspace approaches such as matrix enhancement and matrix pencil (MEMP) [4], 2-D ESPRIT [5], improved multidimensional folding (IMDF) [6], [7], and the methods proposed in [8], [9], (iii) sparse-based algorithms [10]. It is generally admitted that these methods yield accurate estimates at high SNR and/or when the frequencies are well separated. Statistical performances of some of these methods have been studied in the case of undamped sinusoids [6], [7]. Recently, analytical performances of tensor-based ESPRIT-type algorithms have been assessed for undamped signals [11].

In this paper, we focus our attention on the 2-D ESPRIT algorithm of [5]. In sensor array processing, this approach can be used to address the case of a single snapshot via spatial smoothing [8]. The performance of 2-D ESPRIT depends on the shape of the Hankel-block-Hankel (HbH) matrix constructed from 2-D data. To our knowledge, no theoretical study has yet been conducted (especially for damped signals) to optimally choose parameters defining the HbH matrix.

b) Contributions: The main contribution consists in the derivation of closed-form expressions of the variance of the complex modes, frequencies and damping factors estimates

in case of 2-D damped single-tone signals. These expressions are used to define the optimal size of the sub-windows used in the construction of the HbH matrix. We also propose to use a fast algorithm to compute the SVD of the HbH matrix, which reduces the computational complexity of 2-D ESPRIT for large signals.

c) Organisation of the paper: In Section II, we introduce notation, present the 2-D modal retrieval problem and recall the 2-D ESPRIT algorithm. In Section III, a first-order perturbation analysis for 2D-ESPRIT is performed. In Section IV, the single tone case is analyzed and the optimal parameters for the construction of the HbH matrix are discussed. In Section V, computer results are presented to verify the theoretical expressions. We also discuss the complexity of the SVD.

II. PARAMETER ESTIMATION USING 2-D ESPRIT

A. Signal model

The classical model for 2-D modal signals is the superposition of 2-D damped complex sinusoids in noise. In other words, we observe

$$\tilde{y}(m_1, m_2) = \sum_{r=1}^R c_r a_r^{m_1} b_r^{m_2} + e(m_1, m_2) \quad (1)$$

for $m_1 = 0, \dots, M_1 - 1$ and $m_2 = 0, \dots, M_2 - 1$, where $a_r = e^{-\alpha_{a,r} + j\omega_{a,r}}$ are the modes of the first dimension and $b_r = e^{-\alpha_{b,r} + j\omega_{b,r}}$ are those of the second dimension. $\{\alpha_{a,r}, \alpha_{b,r}\}_{r=1}^R$ are damping factors, $\{\omega_{a,r} = 2\pi\nu_{a,r}\}_{r=1}^R$ and $\{\omega_{b,r} = 2\pi\nu_{b,r}\}_{r=1}^R$ are angular frequencies and $\{c_r\}_{r=1}^R$ are complex amplitudes; $e(m_1, m_2)$ is a zero-mean complex Gaussian white noise with variance σ_e^2 and mutually independent components in all dimensions. The problem is to estimate $\{a_r, b_r, c_r\}_{r=1}^R$ from the observed signal $\tilde{y}(m_1, m_2)$. In this paper, the tilde ($\tilde{\cdot}$) is used for noisy quantities. We also denote by $y(m_1, m_2)$ the noiseless signal.

B. 2-D ESPRIT algorithm

Define the HbH matrix

$$\mathbf{H} = \begin{bmatrix} \mathbf{H}_0 & \mathbf{H}_1 & \dots & \mathbf{H}_{K_1-1} \\ \mathbf{H}_1 & \mathbf{H}_2 & \dots & \mathbf{H}_{K_1} \\ \vdots & \vdots & \ddots & \vdots \\ \mathbf{H}_{L_1-1} & \mathbf{H}_{L_1} & \dots & \mathbf{H}_{M_1-1} \end{bmatrix}, \quad (2)$$

where each block \mathbf{H}_{m_1} is an $L_2 \times K_2$ Hankel matrix

$$\mathbf{H}_{m_1} = \begin{bmatrix} y(m_1, 0) & y(m_1, 0) & \dots & y(m_1, K_2-1) \\ y(m_1, 1) & y(m_1, 2) & \dots & y(m_1, K_2) \\ \vdots & \vdots & \ddots & \vdots \\ y(m_1, L_2-1) & y(m_1, L_2) & \dots & y(m_1, M_2-1) \end{bmatrix} \quad (3)$$

This work is funded by the European Research Council under the Seventh Framework Programme FP7/2007–2013 Grant Agreement no. 320594, DECODA project.

S. Sahnoun, K. Usevich and P. Comon are with CNRS, Gipsa-Lab, F-38000 Grenoble, France (e-mail: firstname.name@gipsa-lab.grenoble-inp.fr).

for $m_1 = 0, \dots, M_1 - 1$. We shall also denote $\tilde{\mathbf{H}}$ and $\tilde{\mathbf{H}}_{m_1}$ the noisy versions built upon noisy observations $\tilde{y}(m_1, m_2)$. Then 2-D ESPRIT algorithm [5] can be summarized as follows:

- Choose L_1, L_2 and set $K_1 = M_1 - L_1 + 1, K_2 = M_2 - L_2 + 1$.
- Construct the HbH matrix $\tilde{\mathbf{H}}$ with $L_1 \times K_1$ blocks, in the same format as in (2). It can be verified that its noiseless part can be written as

$$\mathbf{H} = \left(\mathbf{A}^{(L_1)} \odot \mathbf{B}^{(L_2)} \right) \text{Diag}(\mathbf{c}) \left(\mathbf{A}^{(K_1)} \odot \mathbf{B}^{(K_2)} \right)^{\top} \quad (4)$$

where \odot denotes the Khatri-Rao product, \cdot^{\top} denotes the transposition, $\mathbf{A}^{(P)}$ (resp. $\mathbf{B}^{(P)}$) denotes the Vandermonde matrix with P rows and R columns, containing coefficients a_r^p (resp. b_r^p), $p \in \{0, \dots, P - 1\}$, and $P \in \{L_1, L_2, K_1, K_2\}$. $\text{Diag}(\mathbf{c})$ is a diagonal $R \times R$ matrix containing coefficients c_r .

- Perform the SVD of $\tilde{\mathbf{H}}$, and form the matrix $\tilde{\mathbf{U}}_s \in \mathbb{C}^{L_1 L_2 \times R}$ of the R dominant left singular vectors.
- Compute the matrices $\tilde{\mathbf{F}}_1$ and $\tilde{\mathbf{F}}_2$ such that:

$$\mathbf{F}_1 = (\tilde{\mathbf{U}}_s^{\dagger})^{\dagger} \tilde{\mathbf{U}}_s, \quad \mathbf{F}_2 = (\tilde{\mathbf{U}}_s^{\dagger})^{\dagger} \tilde{\mathbf{U}}_s, \quad (5)$$

where \cdot^{\dagger} denotes the pseudoinverse, and for a matrix

$$\mathbf{X} = \begin{bmatrix} \mathbf{x}_1 \\ \vdots \\ \mathbf{x}_{L_1} \end{bmatrix} \in \mathbb{C}^{L_1 L_2 \times N}, \quad \text{with } \mathbf{x}_k \in \mathbb{C}^{L_2 \times N},$$

matrices $\underline{\mathbf{X}}, \overline{\mathbf{X}} \in \mathbb{C}^{(L_1-1)L_2 \times N}$, $\underline{\underline{\mathbf{X}}}, \overline{\overline{\mathbf{X}}} \in \mathbb{C}^{L_1(L_2-1) \times N}$ are defined as

$$\underline{\mathbf{X}} = \begin{bmatrix} \mathbf{x}_1 \\ \vdots \\ \mathbf{x}_{L_1-1} \end{bmatrix}, \quad \overline{\mathbf{X}} = \begin{bmatrix} \mathbf{x}_2 \\ \vdots \\ \mathbf{x}_{L_1} \end{bmatrix}, \quad \underline{\underline{\mathbf{X}}} = \begin{bmatrix} \underline{\mathbf{x}}_1 \\ \vdots \\ \underline{\mathbf{x}}_{L_1} \end{bmatrix}, \quad \overline{\overline{\mathbf{X}}} = \begin{bmatrix} \overline{\mathbf{x}}_1 \\ \vdots \\ \overline{\mathbf{x}}_{L_1} \end{bmatrix},$$

where $\underline{\cdot}$ (resp. $\overline{\cdot}$) removes the last (resp. first) row.

- Compute a diagonalizing matrix $\tilde{\mathbf{T}}$ for a linear combination $\tilde{\mathbf{K}} = \beta \tilde{\mathbf{F}}_1 + (1 - \beta) \tilde{\mathbf{F}}_2$:

$$\tilde{\mathbf{K}} = \tilde{\mathbf{T}} \tilde{\mathbf{D}}_{\boldsymbol{\eta}} \tilde{\mathbf{T}}^{-1}, \quad (6)$$

where β is a complex parameter and $\tilde{\mathbf{D}}_{\boldsymbol{\eta}} = \text{Diag}(\tilde{\boldsymbol{\eta}})$. In the noiseless case, $\eta_r = \beta a_r + (1 - \beta) b_r$. Hence, β should be selected so that elements of $\boldsymbol{\eta}$ are distinct. In [5] β was fixed to 8 in simulations. Later, a selection technique for β was proposed in [7].

- Apply the transformation $\tilde{\mathbf{T}}$ to $\tilde{\mathbf{F}}_1$ and $\tilde{\mathbf{F}}_2$:

$$\tilde{\mathbf{D}}_{\mathbf{a}} = \tilde{\mathbf{T}}^{-1} \tilde{\mathbf{F}}_1 \tilde{\mathbf{T}} \quad \text{and} \quad \tilde{\mathbf{D}}_{\mathbf{b}} = \tilde{\mathbf{T}}^{-1} \tilde{\mathbf{F}}_2 \tilde{\mathbf{T}}. \quad (7)$$

- Extract a_r, b_r from $\text{diag}(\tilde{\mathbf{D}}_{\mathbf{a}})$ and $\text{diag}(\tilde{\mathbf{D}}_{\mathbf{b}})$.

The 2-D ESPRIT method does not require a pairing step. Indeed, the (r, r) element of $\tilde{\mathbf{D}}_{\mathbf{a}}$ corresponds to the same 2-D signal component as the (r, r) element of $\tilde{\mathbf{D}}_{\mathbf{b}}$. Hence, 2-D ESPRIT can estimate the parameters in the presence of identical modes in the dimensions.

III. ANALYSIS OF THE 2-D ESPRIT METHOD

A. Perturbation of signal subspace \mathbf{U}_s

The SVD of the noiseless HbH matrix \mathbf{H} is given by:

$$\mathbf{H} = \mathbf{U}_s \boldsymbol{\Sigma}_s \mathbf{V}_s^{\text{H}} + \mathbf{U}_n \boldsymbol{\Sigma}_n \mathbf{V}_n^{\text{H}},$$

where $\boldsymbol{\Sigma}_n = \mathbf{0}$ and \cdot^{H} denotes the Hermitian transposition. The perturbed $\tilde{\mathbf{H}}$ is expressed as

$$\tilde{\mathbf{H}} = \mathbf{H} + \Delta \mathbf{H},$$

whose subspace decomposition is given by

$$\tilde{\mathbf{H}} = \tilde{\mathbf{U}}_s \tilde{\boldsymbol{\Sigma}}_s \tilde{\mathbf{V}}_s^{\text{H}} + \tilde{\mathbf{U}}_n \tilde{\boldsymbol{\Sigma}}_n \tilde{\mathbf{V}}_n^{\text{H}}. \quad (8)$$

We use the following lemma on the first-order approximation.

Lemma 1 ([12], [13]): First order approximations of the perturbations $\tilde{\mathbf{U}}_s - \mathbf{U}_s$, $\tilde{\mathbf{V}}_s - \mathbf{V}_s$ and $\tilde{\boldsymbol{\Sigma}}_s - \boldsymbol{\Sigma}_s$ are given by

$$\Delta \mathbf{U}_s = \mathbf{U}_n \mathbf{U}_n^{\text{H}} \Delta \mathbf{H} \mathbf{V}_s \boldsymbol{\Sigma}_s^{-1}, \quad (9)$$

$$\Delta \mathbf{V}_s^{\text{H}} = \boldsymbol{\Sigma}_s^{-1} \mathbf{U}_s^{\text{H}} \Delta \mathbf{H} \mathbf{V}_n \mathbf{V}_n^{\text{H}}, \quad (10)$$

$$\Delta \boldsymbol{\Sigma}_s = \mathbf{U}_s^{\text{H}} \Delta \mathbf{H} \mathbf{V}_s. \quad (11)$$

B. Perturbations of the matrices $\mathbf{F}_1, \mathbf{F}_2$ and \mathbf{K}

From (5), we have $\tilde{\mathbf{U}}_s^{\dagger} \tilde{\mathbf{F}}_1 = \tilde{\mathbf{U}}_s^{\dagger}$, which is written also as $(\tilde{\mathbf{U}}_s^{\dagger} + \Delta \tilde{\mathbf{U}}_s^{\dagger})(\mathbf{F}_1 + \Delta \mathbf{F}_1) = \tilde{\mathbf{U}}_s^{\dagger} + \Delta \tilde{\mathbf{U}}_s^{\dagger}$. By canceling $\tilde{\mathbf{U}}_s^{\dagger} \mathbf{F}_1$ and $\tilde{\mathbf{U}}_s^{\dagger}$, and neglecting $\Delta \tilde{\mathbf{U}}_s^{\dagger} \Delta \mathbf{F}_1$, we get that up to first order

$$\Delta \mathbf{F}_1 = (\tilde{\mathbf{U}}_s^{\dagger})^{\dagger} (\Delta \tilde{\mathbf{U}}_s^{\dagger} - \Delta \tilde{\mathbf{U}}_s^{\dagger} \mathbf{F}_1). \quad (12)$$

Similarly, the first-order perturbation $\Delta \mathbf{F}_2$ is given by:

$$\Delta \mathbf{F}_2 = (\tilde{\mathbf{U}}_s^{\dagger})^{\dagger} (\Delta \tilde{\mathbf{U}}_s^{\dagger} - \Delta \tilde{\mathbf{U}}_s^{\dagger} \mathbf{F}_2), \quad (13)$$

and the perturbation of the matrix \mathbf{K} defined in the previous section eventually takes the form: $\Delta \mathbf{K} = \beta \Delta \mathbf{F}_1 + (1 - \beta) \Delta \mathbf{F}_2$.

IV. SINGLE-TONE CASE

In this section, we calculate the perturbations of the parameter estimates for the signal $y(m_1, m_2) = ca^{m_1} b^{m_2}$.

A. Basic expressions

Let \mathbf{u} be the first left singular vector of \mathbf{H} . Then (5) becomes

$$\mathbf{F}_1 = \underline{\mathbf{u}} \underline{\mathbf{u}}^{\dagger}, \quad \mathbf{F}_2 = \underline{\underline{\mathbf{u}}} \underline{\underline{\mathbf{u}}}^{\dagger}. \quad (14)$$

Since, for a single tone, \mathbf{F}_1 and \mathbf{F}_2 are just scalars, we have that $a = \mathbf{F}_1$ and $b = \mathbf{F}_2$, from which it follows that

$$\begin{cases} \Delta a = \frac{1}{\|\underline{\mathbf{u}}\|^2} \underline{\mathbf{u}}^{\text{H}} (\Delta \underline{\mathbf{u}} - a \Delta \underline{\mathbf{u}}), \\ \Delta b = \frac{1}{\|\underline{\underline{\mathbf{u}}}\|^2} \underline{\underline{\mathbf{u}}}^{\text{H}} (\Delta \underline{\underline{\mathbf{u}}} - b \Delta \underline{\underline{\mathbf{u}}}). \end{cases} \quad (15)$$

Let $c = |c| e^{j2\pi\phi}$. From (4), \mathbf{H} can be written as

$$\mathbf{H} = c \left(\mathbf{a}^{(L_1)} \boxtimes \mathbf{b}^{(L_2)} \right) \left(\mathbf{a}^{(K_1)} \boxtimes \mathbf{b}^{(K_2)} \right)^{\top},$$

which implies that an SVD $\mathbf{H} = \sigma \mathbf{u} \mathbf{v}^{\text{H}}$ is given by

$$\sigma = |c| \sqrt{h_u h_v},$$

$$\mathbf{u} = \frac{e^{j2\pi\phi}}{\sqrt{h_u}} \left(\mathbf{a}^{(L_1)} \boxtimes \mathbf{b}^{(L_2)} \right), \quad \mathbf{v} = \frac{1}{\sqrt{h_v}} \left(\mathbf{a}^{*(K_1)} \boxtimes \mathbf{b}^{*(K_2)} \right),$$

$$h_u = \|\mathbf{a}^{(L_1)}\|^2 \|\mathbf{b}^{(L_2)}\|^2, \quad h_v = \|\mathbf{a}^{(K_1)}\|^2 \|\mathbf{b}^{(K_2)}\|^2,$$

where for $x \in \mathbb{C}$ we define $\mathbf{x}^{(L)} = [1, x, \dots, x^{(L-1)}]^{\top}$, $(*)$ denotes the elementwise conjugation, and \boxtimes is the Kronecker product of matrices (vectors are one-column matrices).

B. Expressions for the first-order perturbations

Now, by replacing expressions in (15) by the first-order perturbation (9), we obtain

$$\begin{aligned}\Delta a &= \frac{1}{\sigma \|\underline{\mathbf{u}}\|^2} \underline{\mathbf{u}}^H (\overline{\mathbf{I}} - a_1 \underline{\mathbf{I}}) \mathbf{U}_n \mathbf{U}_n^H \Delta \mathbf{H} \mathbf{v} \\ &= \frac{1}{\sigma \|\underline{\mathbf{u}}\|^2} \left(\underline{\mathbf{u}}^H (\overline{\mathbf{I}} (\mathbf{I} - \mathbf{u} \mathbf{u}^H) - a_1 \underline{\mathbf{I}} (\mathbf{I} - \mathbf{u} \mathbf{u}^H)) \Delta \mathbf{H} \mathbf{v} \right) \\ &= \frac{1}{\sigma \|\underline{\mathbf{u}}\|^2} \left(\underline{\mathbf{u}}^H (\overline{\mathbf{I}} - \overline{\mathbf{u}} \mathbf{u}^H - a_1 \underline{\mathbf{I}} + \overline{\mathbf{u}} \mathbf{u}^H) \Delta \mathbf{H} \mathbf{v} \right) \\ &= \frac{1}{\sigma \|\underline{\mathbf{u}}\|^2} \left(\underline{\mathbf{u}}^H (\overline{\mathbf{I}} - a_1 \underline{\mathbf{I}}) \Delta \mathbf{H} \mathbf{v} \right),\end{aligned}$$

where \mathbf{I} is the $L_1 L_2 \times L_1 L_2$ identity matrix.

Next, the matrices $\overline{\mathbf{I}}$ and $\underline{\mathbf{I}}$ can be first expressed as

$$\overline{\mathbf{I}} = \overline{\mathbf{I}}_{L_1} \boxtimes \mathbf{I}_{L_2} \quad \text{and} \quad \underline{\mathbf{I}} = \underline{\mathbf{I}}_{L_1} \boxtimes \mathbf{I}_{L_2},$$

where under- and over-bars are defined in Section II. Hence, in particular

$$\underline{\mathbf{u}} = \frac{e^{j2\pi\phi}}{\sqrt{h_u}} (\mathbf{a}^{(L_1-1)} \boxtimes \mathbf{b}^{(L_1)}).$$

Second, since $\Delta \mathbf{H}$ is a Hankel-block-Hankel matrix for the noise term $e(m_1, m_2)$, the product $\Delta \mathbf{H} \mathbf{v}$ can be written as the two-dimensional convolution, which yields

$$\Delta \mathbf{H} \mathbf{v} = \frac{1}{\sqrt{h_v}} (\mathbf{G}_{a^*}^{(L_1, K_1)} \boxtimes \mathbf{G}_{b^*}^{(L_2, K_2)}) \mathbf{e},$$

where \mathbf{e} is the vectorized noise term

$$\mathbf{e} = [e(0, 0), \dots, e(0, M_2 - 1), \dots, e(M_1 - 1, 0), \dots, e(M_1 - 1, M_2 - 1)]^T,$$

and for x , the matrix $\mathbf{G}_x^{(L, K)}$ is the convolution matrix

$$\mathbf{G}_x^{(L, K)} = \begin{bmatrix} 1 & x & \dots & x^{K-1} & & \\ & \ddots & \ddots & \ddots & \ddots & \\ & & 1 & x & \dots & x^{K-1} \end{bmatrix} \in \mathbb{C}^{L \times (K+L-1)},$$

where the blank elements denote zeros. Hence,

$$\begin{aligned}\Delta a &= \frac{1}{\sigma \sqrt{h_v}} \cdot \frac{\|\mathbf{a}^{(L_1)}\|^2}{\|\mathbf{a}^{(L_1-1)}\|^2} \cdot \frac{e^{-j2\pi\phi} (\mathbf{a}^{(L_1-1)} \boxtimes \mathbf{b}^{(L_1)})^H}{\sqrt{h_u}} \\ &\cdot (\overline{\mathbf{I}}_{L_1} \boxtimes \mathbf{I}_{L_2} - a_1 \underline{\mathbf{I}}_{L_1} \boxtimes \mathbf{I}_{L_2}) (\mathbf{G}_{a^*}^{(L_1, K_1)} \boxtimes \mathbf{G}_{b^*}^{(L_2, K_2)}) \mathbf{e} \\ &= \frac{e^{-j2\pi\phi}}{\sigma \sqrt{h_u h_v}} \cdot \frac{\|\mathbf{a}^{(L_1)}\|^2}{\|\mathbf{a}^{(L_1-1)}\|^2} \\ &\left(((\mathbf{a}^{(L_1-1)})^H (\overline{\mathbf{I}}_{L_1} - a_1 \underline{\mathbf{I}}_{L_1}) \mathbf{G}_{a^*}^{(L_1, K_1)}) \boxtimes ((\mathbf{b}^{(L_1)})^H \mathbf{G}_{b^*}^{(L_2, K_2)}) \right) \mathbf{e}.\end{aligned}$$

C. Expressions for the moments of the perturbations

Since \mathbf{e} is zero-mean, we have that $\mathbb{E}\{\Delta a\} = 0$. Next, as $\mathbb{E}\{\mathbf{e} \mathbf{e}^H\} = \sigma_e^2 \mathbf{I}_{M_1 M_2}$, the variance of Δa can be found as

$$\mathbb{E}\{|\Delta a|^2\} = \frac{\sigma_e^2}{|c|^2} f(L_1, M_1, a) g(L_2, M_2, b), \quad (16)$$

where the functions $f(L, M, x)$ and $g(L, M, x)$ are defined as

$$f(L, M, x) = \frac{\|(\mathbf{x}^{(L-1)})^H (\overline{\mathbf{I}}_L - x \underline{\mathbf{I}}_L) \mathbf{G}_{x^*}^{(L, K)}\|^2}{\|\mathbf{x}^{(K)}\|^4 \|\mathbf{x}^{(L-1)}\|^4},$$

$$g(L, M, x) = \frac{\|(\mathbf{x}^{(L)})^H \mathbf{G}_{x^*}^{(L, K)}\|^2}{\|\mathbf{x}^{(L)}\|^4 \|\mathbf{x}^{(K)}\|^4},$$

and $K = M - L + 1$. Similarly, we get

$$\mathbb{E}\{|\Delta b|^2\} = \frac{\sigma_e^2}{|c|^2} f(L_2, M_2, b) g(L_1, M_1, a). \quad (17)$$

It can be verified that the variances of the frequencies and the damping factors are expressed as:

$$\text{var}(\Delta \omega_a) = \text{var}(\Delta \alpha_a) = \frac{\mathbb{E}\{|\Delta a|^2\}}{2|a|^2}, \quad (18)$$

$$\text{var}(\Delta \omega_b) = \text{var}(\Delta \alpha_b) = \frac{\mathbb{E}\{|\Delta b|^2\}}{2|b|^2}. \quad (19)$$

D. Closed form expressions

Our next goal is to give closed-form expressions of $f(L, M, x)$ and $g(L, M, x)$. It is easy to see that

$$(\mathbf{x}^{(L)})^H \mathbf{G}_{x^*}^{(L, K)} = [1, 2x^*, 3x^{*2}, \dots, L_* x^{*(L_*-1)}, \dots, L_* x^{*(M-L_*)}, (L_* - 1)x^{*(M-L_*+1)}, \dots, 2x^{*(M-2)}, x^{*(M-1)}].$$

where $L_* = \min(L, K)$. Next, we have that

$$\begin{aligned} & [(\mathbf{x}^{(L-1)})^H (\overline{\mathbf{I}}_L - x \underline{\mathbf{I}}_L) \mathbf{G}_{x^*}^{(L, K)}]_i = \\ & \begin{cases} (i(1 - |x|^2) - |x|^2) x^{*(i-1)}, & i = 0, \dots, L_{**} - 1, \\ L_{**} (1 - |x|^2) x^{*(i-1)}, & i = L_{**}, \dots, M - L_{**} - 1, \\ ((M - i)(1 - |x|^2) + |x|^2) x^{*(i-1)}, & i = M - L_{**}, \dots, M - 1, \end{cases} \end{aligned}$$

where $L_{**} = \min(L - 1, K)$. In the damped case ($|x| \neq 1$), after tedious calculations, Eq. (22) and (23) can be obtained for $f(L, M, x)$ and $g(L, M, x)$. Detailed derivations will be given in a full-length version of the paper. In the undamped case the expressions are much simpler and are given in (20) and (21). We notice that the functions f and g are symmetric with respect to $L = \frac{M}{2} + 1$ and $L = \frac{M+1}{2}$, respectively.

$$f(L, M, x) = \begin{cases} \frac{2}{K^2(L-1)}, & \text{if } L - 1 \leq \frac{M}{2} \text{ and } |x| = 1 \\ \frac{2}{K(L-1)^2}, & \text{if } L - 1 \geq \frac{M}{2} \text{ and } |x| = 1 \end{cases} \quad (20)$$

$$g(L, M, x) = \begin{cases} \frac{1}{L} - \frac{L^2 - 1}{3LK^2}, & \text{if } L \leq \frac{M+1}{2} \text{ and } |x| = 1 \\ \frac{1}{L} - \frac{K^2 - 1}{3L^2K}, & \text{if } L \geq \frac{M+1}{2} \text{ and } |x| = 1 \end{cases} \quad (21)$$

$$\begin{aligned} f(L, M, x) &= (1 - |x|^2)^3 \times \\ & \begin{cases} \frac{1 + |x|^{2K}}{(1 - |x|^{2K})^2 (1 - |x|^{2(L-1)})}, & \text{if } L - 1 \leq \frac{M}{2} \text{ and } |x| \neq 1 \\ \frac{1 + |x|^{2(L-1)}}{(1 - |x|^{2K})(1 - |x|^{2(L-1)})^2}, & \text{if } L - 1 \geq \frac{M}{2} \text{ and } |x| \neq 1 \end{cases} \end{aligned} \quad (22)$$

$$g(L, M, x) = (1 - |x|^2) \times \begin{cases} \frac{-2L(1-|x|^2)(|x|^{2K} + |x|^{2L})}{(1-|x|^{2L})^2(1-|x|^{2K})^2} + \frac{(1+|x|^{2K})(1+|x|^2)}{(1-|x|^{2L})(1-|x|^{2K})^2}, & \text{if } L \leq \frac{M+1}{2} \text{ and } |x| \neq 1 \\ \frac{-2K(1-|x|^2)(|x|^{2L} + |x|^{2K})}{(1-|x|^{2L})^2(1-|x|^{2K})^2} + \frac{(1+|x|^{2L})(1+|x|^2)}{(1-|x|^{2L})^2(1-|x|^{2K})}, & \text{if } L \geq \frac{M+1}{2} \text{ and } |x| \neq 1 \end{cases} \quad (23)$$

E. Optimal values for L_1 and L_2

In [14], the optimal value of L has been obtained so as to minimize $f(L, M, x)$ (which corresponds to the case of 1-D signals). In the case of 2-D ESPRIT, there are two variables, L_1 and L_2 , but they separate in the expressions of variances. Therefore, the optimal values of L_1 and L_2 are simply given by minimal values of each function, namely f and g .

As discussed in [14], the L that minimizes $f(L, M, x)$ lies between $M/3$ and $M/2$ and approaches $M/2$ as the damping factor of x increases (or if M tends to ∞). These results are shown in Figure 1. Regarding function $g(L, M, x)$, it can be seen from Figure 2 that the minimum is reached for small L . Therefore, the optimal values of L_1 and L_2 minimizing $\text{var}(\Delta\omega_a)$ (resp. $\text{var}(\Delta\omega_b)$) lie between $M/3$ and $M/2$ for L_1 (resp. L_2) and L_2 (resp. L_1) should be chosen as small as possible. This is illustrated by typical examples in Figure 3 (resp. Figure 4). As in [8], the total Mean Square Error (tMSE) is taken to be $\text{tMSE} = \text{var}(\Delta\omega_a) + \text{var}(\Delta\omega_b)$; the tMSE corresponding to Figures 3-4 is plotted in Figure 5.

As indicated by the results shown in Figure 5, for case where damping factors are known to be less than 0.1, the values of L_i that minimize tMSE should be chosen in the intervals $[M_i/4, M_i/2]$.

V. SIMULATIONS

We consider a 2-D damped single-tone signal with parameters $(\alpha_a, \omega_a) = (-0.1, 0.2\pi)$ and $(\alpha_b, \omega_b) = (-0.1, 0.4\pi)$. The SNR is fixed to 40 dB. Figure 6 shows the sample MSE and its theoretical value for ω_1 obtained from 200 Monte Carlo trials with $(M_1, M_2) = (30, 30)$. Since it is difficult to see the difference between the two curves in a 3-D plot, we show only one slice of the 3-D plot corresponding to $L_2 = 4$. We can observe that the theoretical MSEs are close to the estimated ones. In the second example, we repeat the same experiment with $(M_1, M_2) = (100, 100)$ using the fast SVD method. The obtained results are reported in Figure 7, where it can be seen that theoretical MSEs are again close to the estimated ones.

In the third example, the same parameters of the modes are used but the SNR is varying. The parameters (L_1, L_2) are set to $(4, 4)$. The obtained results are depicted in Figure 8. We observe that the theoretical results are almost equal to empirical ones beyond a threshold, which is here -5 dB.

To compute 2D-ESPRIT estimates, we use the fast methods for partial SVD of HbH matrices [15, Sec. 6], where only the first R singular values/vectors are computed. The overall complexity of 2D-ESPRIT becomes $O(RM \log M)$ flops, compared with the complexity $O(L^2K)$ of the naive implementation (where $K = K_1K_2$, $L = L_1L_2$ and $M = M_1M_2$). Hence, optimal or near-optimal values of parameters (for example, $(L_1, L_2) = (M_1/2, M_2/2)$) can be used for large signals.

VI. CONCLUSION

The 2-D ESPRIT algorithm is implemented by storing the $M_1 \times M_2$ data matrix into a HbH matrix with L_1L_2 lines. A perturbation analysis has been carried out, which led to a closed form expression of the variances of first-order perturbations of parameters (damping factors and frequencies). It has then been shown that variables L_1 and L_2 separate in each of these variances. This property enables us to find the intervals for the optimal values of L_i that minimize the variance of the estimates. The optimal values of L_i are different depending on whether we minimize the MSE in each dimension or the total MSE.

REFERENCES

- [1] A. B. Gershman and N. D. Sidiropoulos, *Space-time processing for MIMO communications*. Wiley Online Library, 2005.
- [2] Y. Li, J. Razavilar, and K. J. R. Liu, "A high-resolution technique for multidimensional NMR spectroscopy," *IEEE Transactions on Biomedical Engineering*, vol. 45, no. 1, pp. 78–86, 1998.
- [3] J. Sacchini, W. Steedly, and R. Moses, "Two-dimensional Prony modeling and parameter estimation," *IEEE Trans. Signal Process.*, vol. 41, no. 11, pp. 3127–3137, 1993.
- [4] Y. Hua, "Estimating two-dimensional frequencies by matrix enhancement and matrix pencil," *IEEE Trans. Signal Process.*, vol. 40, no. 9, pp. 2267–2280, 1992.
- [5] S. Rouquette and M. Najim, "Estimation of frequencies and damping factors by two-dimensional ESPRIT type methods," *IEEE Trans. Signal Process.*, vol. 49, no. 1, pp. 237–245, 2001.
- [6] J. Liu and X. Liu, "An eigenvector-based approach for multidimensional frequency estimation with improved identifiability," *IEEE Trans. Signal Process.*, vol. 54, no. 12, pp. 4543–4556, 2006.
- [7] J. Liu, X. Liu, and X. Ma, "Multidimensional frequency estimation with finite snapshots in the presence of identical frequencies," *IEEE Transactions on Signal Processing*, vol. 55, pp. 5179–5194, 2007.
- [8] M. Haardt, F. Roemer, and G. Del Galdo, "Higher-order SVD-based subspace estimation to improve the parameter estimation accuracy in multidimensional harmonic retrieval problems," *IEEE Trans. Signal Process.*, vol. 56, no. 7, pp. 3198–3213, 2008.
- [9] L. Huang, Y. Wu, H. So, Y. Zhang, and L. Huang, "Multidimensional sinusoidal frequency estimation using subspace and projection separation approaches," *IEEE Trans. Signal Process.*, vol. 60, no. 10, pp. 5536–5543, 2012.
- [10] S. Sahnoun, E.-H. Djermoune, C. Soussen, and D. Brie, "Sparse multidimensional modal analysis using a multigrid dictionary refinement," *EURASIP J. Adv. Signal Process.*, March 2012.
- [11] F. Roemer, M. Haardt, and G. Del Galdo, "Analytical performance assessment of multi-dimensional matrix-and tensor-based ESPRIT-type algorithms," *IEEE Trans. Signal Process.*, vol. 62, no. 10, pp. 2611–2625, 2014.
- [12] F. Li, H. Liu, and R. J. Vaccaro, "Performance analysis for DOA estimation algorithms: unification, simplification, and observations," *Aerospace and Electronic Systems, IEEE Transactions on*, vol. 29, no. 4, pp. 1170–1184, 1993.
- [13] Z. Xu, "Perturbation analysis for subspace decomposition with applications in subspace-based algorithms," *IEEE Trans. Signal Process.*, vol. 50, no. 11, pp. 2820–2830, 2002.
- [14] E.-H. Djermoune and M. Tomczak, "Perturbation analysis of subspace-based methods in estimating a damped complex exponential," *IEEE Trans. Signal Process.*, vol. 57, no. 11, pp. 4558–4563, 2009.
- [15] N. Golyandina, A. Korobeynikov, A. Shlemov, and K. Usevich, "Multivariate and 2D extensions of Singular Spectrum Analysis with the Rssa package," *Journal of Statistical Software*, vol. 67, no. 1, 2015.

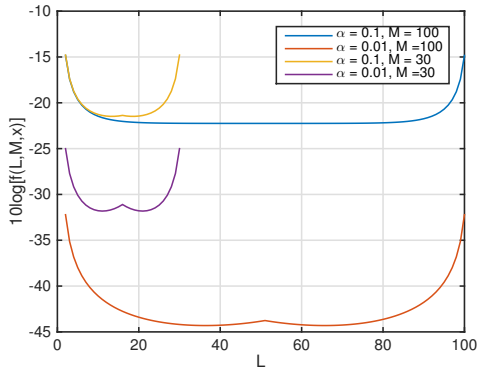


Fig. 1. Behavior of function $f(L, M, x)$ as a function of L for different values of M and damping factors.

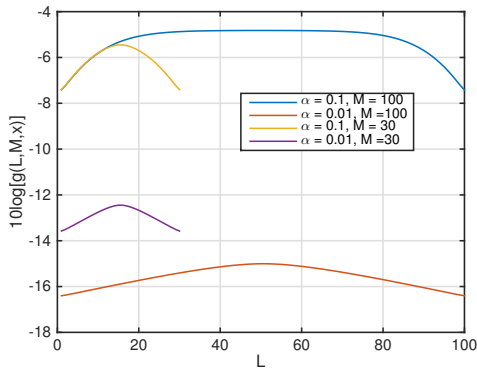


Fig. 2. Behavior of function $g(L, M, x)$ as a function of L for different values of M and damping factors.

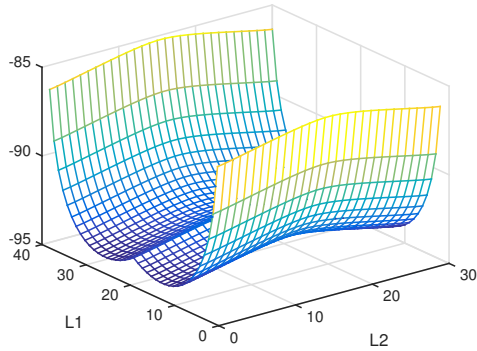


Fig. 3. Variance of $\Delta\omega_a$ as a function of L_1 and L_2

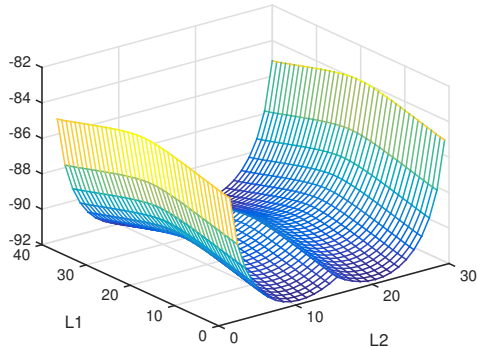


Fig. 4. Variance of $\Delta\omega_b$ as a function of L_1 and L_2

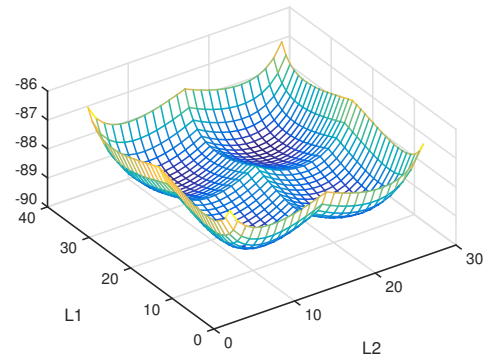


Fig. 5. tMSE as a function of L_1 and L_2

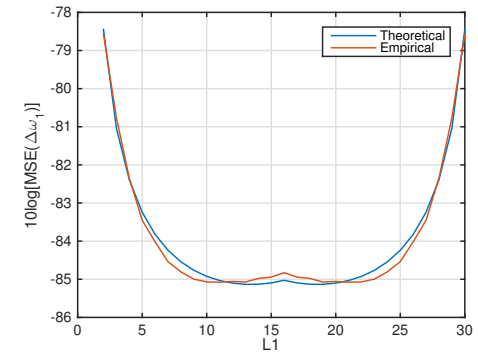


Fig. 6. Theoretical and empirical MSEs for 2-D ESPRIT versus L_1 , ($L_2 = 4$). $(\alpha_a, \omega_a) = (-0.1, 0.2\pi)$, $(\alpha_b, \omega_b) = (-0.1, 0.4\pi)$, $(M_1, M_2) = (30, 30)$, SNR = 40 dB.

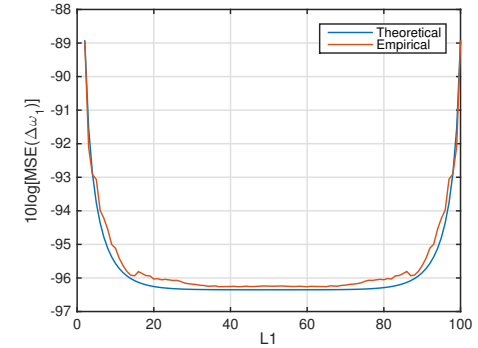


Fig. 7. Theoretical and empirical MSEs for 2-D ESPRIT (fast SVD) versus L_1 , ($L_2 = 4$). $(\alpha_a, \omega_a) = (-0.1, 0.2\pi)$, $(\alpha_b, \omega_b) = (-0.1, 0.4\pi)$, $(M_1, M_2) = (100, 100)$, SNR = 40 dB.

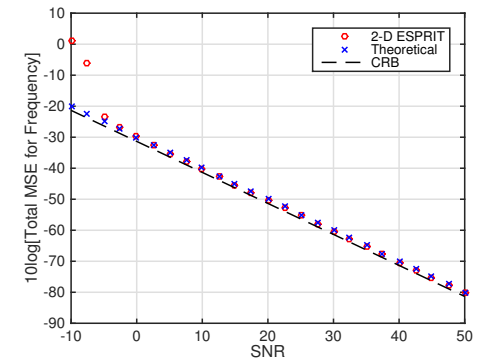


Fig. 8. Theoretical and empirical tMSEs for 2-D ESPRIT versus SNR. $(L_1, L_2) = (4, 4)$. $(\alpha_a, \omega_a) = (-0.1, 0.2\pi)$, $(\alpha_b, \omega_b) = (-0.1, 0.4\pi)$, $(M_1, M_2) = (10, 10)$.